Photosynthetic Oxygen Evolution in Mesoporous Silica Material: Adsorption of Photosystem II Reaction Center Complex into 23 nm Nanopores in SBA

ARTICLE *in* LANGMUIR · JANUARY 2011

Impact Factor: 4.46 · DOI: 10.1021/la1032916 · Source: PubMed

8 AUTHORS, INCLUDING:

Tomoyasu Noji
Nagoya Institute of Technology
18 PUBLICATIONS **60** CITATIONS

SEE PROFILE

Shigeru Itoh
Nagoya University
222 PUBLICATIONS **4,121** CITATIONS

SEE PROFILE

Langmuir
Article
pubs.acs.org/Langmuir

Photosynthetic Oxygen Evolution in Mesoporous Silica Material: Adsorption of Photosystem II Reaction Center Complex into 23 nm Nanopores in SBA

Tomoyasu Noji,[†] Chihiro Kamidaki,[†] Keisuke Kawakami,[‡] Jian-Ren Shen,[‡] Tsutomu Kajino,[§] Yoshiaki Fukushima,[§] Takeshi Sekitoh,[⊥] and Shigeru Itoh*[,†]

[†]*Division of Material Science (Physics), Graduate School of Science, Nagoya University, Furo-cho, Chikusa-ku Nagoya, Aichi 464-8602, Japan,* [‡]*Division of Bioscience, Graduate School of Natural Science and Technology/Faculty of Science, Okayama University, Okayama 700-8530, Japan,* [§]*Toyota Central R&D Lab., Inc., Yokomichi Nagakute, Aichi 480-1192, Japan, and* [⊥]*Advanced Material Engineering Div., Toyota Motor Co., Toyota-cho, Toyota, Aichi, 471-8572, Japan*

Received August 18, 2010. Revised Manuscript Received November 26, 2010

An oxygen-evolving photosynthetic reaction center complex (PSII) was adsorbed into nanopores in SBA, a mesoporous silica compound. We purified the dimer of PSII complex from a thermophilic cyanobacterium, *Thermosynechococcus vulcanus*, which grows optimally at 57 °C. The thermally stable PSII dimeric complex has a diameter of 20 nm and a molecular mass of 756 kDa and binds more than 60 chlorophylls. The SBA particles, with average internal pore diameters of 15 nm (SBA_{15}) and 23 nm (SBA_{23}), adsorbed 4.7 and 15 mg of PSII/g SBA, respectively. Measurement with a confocal laser-scanning microscope indicated the adsorption of PSII to the surface and the inner space of the SBA_{23} particles, indicating the adsorption of PSII into the 23 nm silica nanopores. PSII did not bind to the inner pores of SBA_{15}. PSII bound to SBA_{23} showed the high and stable activity of a photosynthetic oxygen-evolving reaction, indicating the light-driven electron transport from water to the quinone molecules added in the outer medium. The PSII−SBA conjugate can be a new material for photosensors and artificial photosynthetic systems.

Introduction

Mesoporous silica materials, which have inner pores with diameters of nanometer sizes, have been used to adsorb various organic molecules in order to provide new platforms of their functions.[1] Immobilization of large molecules such as chlorophyll (with a molecular mass of 0.9 kDa[2−4]) or soluble proteins with a molecular mass of 44−250 kDa[5−10] in mesoporous silica materials often increases their molecular stability, as shown in the case of chlorophyll *a* in a folded silica mesoporous material (FSM).[3,4] A recent differential interference contrast microscopy study directly indicated the distribution of a fluorescence-labeled enzyme inside nanopores in FSM.[11−13] The incorporation of a large hydrophobic membrane protein complex was also reported for the photosynthetic light-harvesting protein LH2,[14] a supramolecular complex (129 kDa) made of 9 proteins, 27 bacteriochlorophyll (BChl) *a*, and 9 carotenoid pigments. The thermally stable LH2 complex that was isolated from a thermophilic purple photosynthetic bacterium acquired higher thermal stability inside FSM. A recent study reported that the bacterial type photosynthetic reaction center complex (137 kDa) isolated from the same species of bacterium was fully photoactive inside FSM and acquired higher thermal stability.[15] The interior of the mesoporous silica, therefore, seems to be suitable for the incorporation of the membrane proteins. In this study, we incorporated the dimeric form of the photosystem II reaction center core complex (PSII), which is large in molecular mass (756 kDa) and size (20 nm), into another type of mesoporous silica material SBA,[16] which has large, 23 nm diameter inner pores, to realize photosynthetic light-induced oxygen evolution inside silica nanopores, i.e., the extraction of electrons from water and their transfer to the artificial organic mediator molecules in the outer medium.

Oxygen-evolving photosynthesis, which seems to have evolved first in cyanobacteria and then transferred into plants, has changed Earth's atmosphere[17,18] by using water as the electron source and evolving oxygen as a byproduct. In plant- and cyanobacterial-type photosynthesis, solar energy is captured by chlorophylls in the two types of pigment−protein complexes (photosystems I and II, designated PSI and PSII, respectively)

*To whom correspondence should be addressed. E-mail: itoh@bio.phys.nagoya-u.ac.jp.

(1) Yiu, H. H. P.; Wright, P. A. *J. Mater. Chem.* **2005**, *15*, 3690–3700.
(2) Itoh, T.; Yano, K.; Kajino, T.; Itoh, S.; Shibata, Y.; Mino, H.; Miyamoto, R.; Inada, Y.; Iwai, S.; Fukushima, Y. *J. Phys. Chem. B* **2004**, *108*, 13683–13687.
(3) Itoh, T.; Yano, K.; Inada, Y.; Fukushima, Y. *J. Am. Chem. Soc*. **2002**, *124*, 13437–13441.
(4) Itoh, T.; Yano, K.; Inada, Y.; Fukushima, Y. *J. Mater. Chem.* **2002**, *12*, 3275–3277.
(5) Takahashi, H.; Li, B.; Sasaki, T.; Miyazaki, C.; Kajino, T.; Inagaki, S. *Chem. Mater*. **2000**, *12*, 3301–3305.
(6) Li, B.; Takahashi, H. *Biotechnol. Lett*. **2000**, *22*, 1953–1958.
(7) Pandya, P. H.; Jasra, R. V.; Newalkar, B. L.; Bhatt, P. N. *Microporous Mesoporous Mater*. **2005**, *77*, 67–77.
(8) Zhang, X.; Guan, R. F.; Wu, D. Q.; Chan, K. Y. *J. Mol. Catal. B: Enzym.* **2005**, *33*, 43–50.
(9) Wang, Y. J.; Caruso, F. *Chem. Mater*. **2005**, *17*, 953–961.
(10) Luckarift, H. R.; Spain, J. C.; Naik, R. R.; Stone, M. O. *Nature Biotechnol.* **2004**, *22*, 211–213.
(11) Itoh, T.; Ishii, R.; Matsuura, S.; Hamakawa, S.; Hanaoka, T.; Tsunoda, T.; Mizuguchi, J.; Mizukami, F. *Biochem. Eng. J*. **2009**, *44*, 167–173.
(12) Itoh, T.; Ishii, R.; Matsuura, S.; Mizuguchi, J.; Hamakawa, S.; Hanaoka, T.; Tsunoda, T.; Mizukami, F. *Colloids Surf., B* **2010**, *75*, 478–482.
(13) Matsuura, S.; Ishii, R.; Itoh, T.; Hanaoka, T.; Hamakawa, S.; Tsunoda, T.; Mizukami, F. *Microporous Mesoporous Mater*. **2010**, *127*, 61–66.
(14) Oda, I.; Hirata, K.; Watanabe, S.; Shibata, Y.; Kajino, T.; Fukushima, Y.; Iwai, S.; Itoh, S. *J. Phys. Chem. B* **2006**, *110*, 1114–1120.
(15) Oda, I.; Iwaki, M.; Fujita, D.; Tsutsui, Y.; Ishizaka, S.; Dewa, M.; Nango, M.; Kajino, T.; Fukushima, Y.; Itoh, S. *Langmuir* **2010**, *26*, 13399–13406.
(16) Zhao, D. Y.; Feng, J. L.; Huo, Q. S.; Melosh, N.; Fredrickson, G. H.; Chmelka, B. F.; Stucky, G. D. *Science* **1998**, *279*, 548–552.
(17) Des Marais, D. J. *Science* **2000**, *289*, 1703–1705.
(18) Rye, R.; Holland, H. D. *Am. J. Sci.* **1998**, *298*, 621–672.

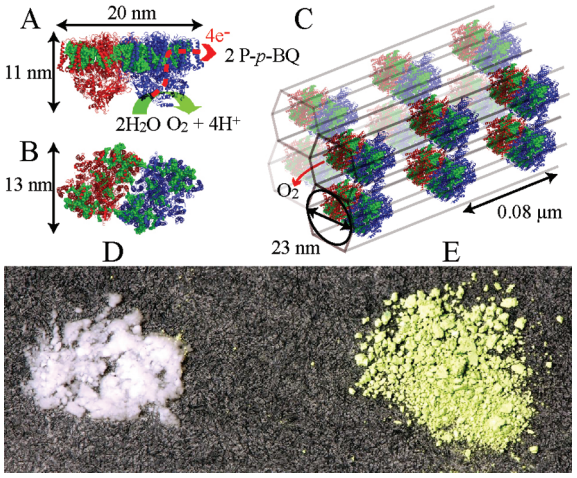

Figure 1. Structure of PSII dimer and electron transfer pathway (A and B), arrangement of PSII inside SBA_{23} (C), and photographic images of SBA_{23} before (D) and after (E) the adsorption of PSII. (A) Side view of the PSII dimer structure with its cytoplasmic side to be top. Electron transfer pathway from water to extraneous P-*p*-BQ is drawn with a red broken line, too. (B) View from the cytoplasmic side of the membrane. (C) Schematic view of the distribution of PSII reaction center complexes in the PSII−SBA_{23} conjugate. Average distances between PSII dimers are assumed to be 80 nm based on the experimental result. (D, E) Images of dry powder of SBA_{23} (D) and PSII−SBA_{23} conjugate (E). The PSII structure was drawn by using a PyMOL software with pdb data files of 3BZ1 and 3BZ2.[20]

and are converted into electrochemical energy to produce ATP and NADPH that are used for CO_2 fixation.[19] PSII performs the light-induced oxygen evolution reaction and transfers electrons from water to plastoquinone in the membrane and PSI produces strong reducing power using electrons supplied by PSII and reduces ferredoxin and $NADP^+$. Plants have large amounts of antenna pigment protein complexes associated with PSI and PSII reaction center complexes; each of them binds about 200 Chls *a*/*b* altogether in antenna and reaction center complexes, to harvest solar energy efficiently, while cyanobacteria have simpler systems with no or only a small amounts of Chl-binding antenna proteins with PSI and PSII. In this study, we purified PSII complex from the cells of a thermophilic cyanobacterium, *Thermosynechococcus vulcanus*, which grows optimally at 57 °C. We introduced its very stable PSII complex into SBA to realize a light-driven reduction of external organic compounds by electrons from water, which is an almost infinite source of electrons.

The structure of the PSII of *T. vulcanus* in its dimer form (Figure 1A) has a size of 20 × 13 × 11 nm and a molecular mass of 756 kDa.[20−22] The PSII monomer in the dimer is made of 20 protein subunits and 35 chlorophyll *a* (Chl *a*) molecules, together with 2 pheophytin *a* molecules, 2 plastoquinone molecules, and 4 atoms of manganese that work for oxygen evolution.[20] A light quantum absorbed by any Chl *a* is transferred to a special pair of Chl *a* (P680) at the center of PSII and initiates the electron transfer to pheophytin *a* and plastoquinone with the quantum efficiency of almost unity.[19] Artificial electron acceptors, such as phenyl-*p*-benzoquinone (P-*p*-BQ), added into the outer medium can accept electrons from plastoquinone, as shown in Figure 1A. Photoproduced $P680^+$ oxidizes H_2O by the function of the manganese complex and liberates O_2. The protein subunits and cofactors are noncovalently bound to each other in the complex[23−28] and are easily dissociated after the isolation of the complex. In this report, we show that the isolated PSII of *T. vulcanus* is highly stable and well adsorbed into the 23 nm silica nanopores in SBA without losing its stability and performs oxygen evolution efficiently.

Materials and Methods

Preparation of SBA, a Mesoporous Material. SBA-15 (designated SBA in this study) with highly ordered two-dimensional honeycomb-like hexagonal silica inner pores were prepared as reported,[16,29] by use of amphiphilic block copolymers as organic structure-directing agents. We prepared two types of SBA with diameters of 23 and 15 nm (hereafter designated SBA_{23} and SBA_{15}, respectively) with average particle sizes of about 4.6 μm. The pore diameter distribution curves were derived from the N_2 adsorption isotherm measurements by the BJH method,[30] as previously described.[14]

Preparation of PSII Dimer Complex of *T. vulcanus*. The PSII dimer complex was purified from cells of a thermophilic cyanobacterium, *T. vulcanus*, grown at 57 °C, as described previously.[31,32] Thylakoid membranes isolated from cells were solubilized with 1% (w/v) sodium *n*-dodecyl-β-D-maltoside (DM). The solubilized mixture was passed through an anion exchange chromatography column two times to purify the PSII dimer complex separately from the PSI and PSII monomer complexes and other proteins. The obtained PSII dimer complex was suspended in 20 mM MES-NaOH (pH 6.0), 20 mM NaCl, 3 mM $CaCl_2$, and 25% (w/v) glycerol (medium A) and then stored in liquid N_2 until use.

Preparation of PSII−SBA or Neutral Red (NR)−SBA Conjugate. *Adsorption of PSII to SBA_{15} or SBA_{23}.* An aliquot of a stock solution of PSII was dissolved in medium A containing 1.0% (w/v) DM at 1.0 mg Chl/mL and was incubated for 5 min on ice. Solubilized PSII was diluted two times by adding the same medium. The smaller molecules were removed by centrifugation with a centrifugal filter unit (Amicon Ultra-15, 50,000 MWCO, Millipore Co., Billerica, MA) three times. The final concentration of the PSII dimer was adjusted to 0.15 mg Chl/mL with medium A containing 0.02% (w/v) DM. SBA particles were added at 20 mg/mL to the PSII-containing medium under gentle stirring at 25 °C, and the mixture was incubated for 0−3 h. Occasionally, the stirring was stopped, and aliquots of the medium were withdrawn and centrifuged at 1000*g* for 1 min to sediment the PSII−SBA conjugate. The amount of PSII adsorbed to SBA was monitored by the absorbance decrease at 673 nm of the supernatant by a double-beam spectrophotometer (UV-3100PC, Shimadzu, Kyoto, Japan) during the stirring. The concentration of PSII on the SBA conjugate was also determined directly by the extraction of chlorophyll.

(19) Nelson, N.; Ben-Shem, A. *Nat. Rev. Mol. Cell Biol.* **2004**, *5*, 971–982.
(20) Guskov, A.; Kern, J.; Gabdulkhakov, A.; Broser, M.; Zouni, A.; Saenger, W. *Nat. Struct. Mol. Biol.* **2009**, *16*, 334–342.
(21) Zouni, A.; Kern, J.; Frank, J.; Hellweg, T.; Behlke, J.; Saenger, W.; Irrgang, K. D. *Biochemistry* **2005**, *44*, 4572–4581.
(22) Kamiya, N.; Shen, J. R. *Proc. Natl. Acad. Sci. U.S.A.* **2003**, *100*, 98–103.
(23) Enami, I.; Okumura, A.; Nagao, R.; Suzuki, T.; Iwai, M.; Shen, J. R. *Photosynth. Res.* **2008**, *98*, 349–363.
(24) Enami, I.; Kitamura, M.; Tomo, T.; Isokawa, Y.; Ohta, H.; Katoh, S. *Biochim. Biophys. Acta, Bioenerg.* **1994**, *1186*, 52–58.
(25) Yamamoto, Y.; Doi, M.; Tamura, N.; Nishimura, M. *FEBS Lett.* **1981**, *133*, 265–268.
(26) Kuwabara, T.; Murata, N. *Plant Cell Physiol.* **1983**, *24*, 741–747.
(27) Ono, T.; Inoue, Y. *FEBS Lett.* **1984**, *166*, 381–384.
(28) Ono, T.; Inoue, Y. *Biochim. Biophys. Acta* **1983**, *723*, 191–201.
(29) Takahashi, H.; Li, B.; Sasaki, T.; Miyazaki, C.; Kajino, T.; Inagaki, S. *Microporous Mesoporous Mater.* **2001**, *44*, 755–762.
(30) Barrett, E. P.; Joyner, L. G.; Halenda, P. P. *J. Am. Chem. Soc.* **1951**, *73*, 373–380.
(31) Kawakami, K.; Iwai, M.; Ikeuchi, M.; Kamiya, N.; Shen, J. R. *FEBS Lett.* **2007**, *581*, 4983–4987.
(32) Shen, J. R.; Kamiya, N. *Biochemistry* **2000**, *39*, 14739–14744.

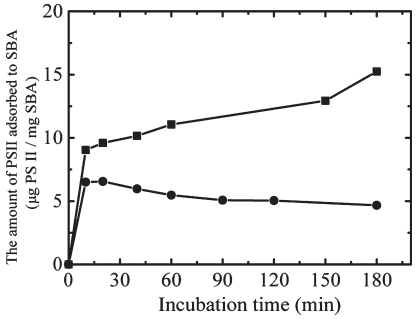

Figure 2. Time courses of adsorption of PSII to SBA_{23} and SBA_{15}. Solid squares and circles represent the cases with SBA_{23} and SBA_{15}, respectively. Dry SBA powder was added to PSII solution under gentle stirring in dark at 25 °C. The decrease in absorbance at 673 nm of PSII in the supernatant was monitored after the precipitation of PSII−SBA conjugates by centrifugation at each point.

Adsorption of Neutral Red (NR) to SBA. 1.0 mg of SBA_{15} or SBA_{23} was added to a 1.0 mL solution containing 0.5 mM NR and 50 mM MES-NaOH (pH 6.5) buffer. The mixture was stirred at 25 °C for 30 min.

Formed PSII−SBA or NR−SBA conjugates were collected by centrifugation at 7000*g* for 1 min using a centrifugal filter unit (Ultrafree-MC filter with a pore size of 0.65 μm; Millipore Co., Billerica, MA) and were diluted with medium A or 50 mM MES-NaOH (pH 6.5) buffer, respectively. This process was repeated three times to remove the free PSII. The NR−SBA conjugate was obtained by the same procedure.

Absorption and Fluorescence Spectrum. Absorption spectra of samples were measured at room temperature by using a double-beam spectrophotometer (UV-3100PC, Shimadzu, Kyoto, Japan). The light scattering from SBA was compensated for by subtracting the absorption spectrum of free SBA. The fluorescence spectrum was measured with a fluorescence spectrophotometer (F-4500, Hitachi, Tokyo, Japan).

Confocal Laser Scanning Microscopy. Imaging of fluorescence from PSII Chl or from NR on single SBA particles was performed with a confocal laser scanning microscope (Nanofinder, Tokyo Instruments, Tokyo, Japan) equipped with a 100×, 1.3 numerical aperture oil-immersion objective lens (Plan Fluor, Nikon, Tokyo, Japan). The stock solution of PSII−SBA conjugate or NR−SBA conjugate was diluted to give 0.2−0.4 mg of SBA/mL by dilution with medium A or 50 mM MES-NaOH (pH 6.5) buffer, respectively. Then, 10 μL of each sample was mounted on a microscope slide and covered with a cover glass. Fluorescence intensities of PSII (peaking at 680 nm) and NR (620 nm) that were excited by a 488 nm Ar laser beam at 1.8 μW (5490ASL-00, Ion Laser Technology, Inc., Tokyo, Japan) were detected by a photomultiplier (R943-02, Hamamatsu Photonics, Hamamatsu, Japan) with and without a red cutoff filter (Toshiba R60, Toshiba, Tokyo, Japan), respectively, after eliminating the excitation laser by a dichroic mirror. The *XY* images were obtained with a unit pixel size of $0.15 \times 0.15\ \mu m^2$ in each case and with a typical accumulation time of 2 or 0.01 s for each pixel in the measurement of the PSII−SBA and NR−SBA conjugates, respectively.

Measurement of Oxygen Evolution. Oxygen evolution was measured at 25 °C using a Clark-type electrode (Rank Brothers, Ltd., Cambridge, England) as reported.[32] Red light from a 550 W halogen lamp through a UV-cut filter and a red-pass filter (Y43 and R-62, respectively, Toshiba, Tokyo, Japan), a heat-cut filter (HA-50, Hoya, Saitama, Japan), an ND filter (10%, Optical Coatings Japan, Tokyo, Japan), and a 14 cm water layer illuminated a 1 cm diameter reaction vessel at 1 mL in the experiments in Figure 3. In all the other measurements like those in Figure 4 and Table 1, the red-pass and neutral density filters were omitted to give the white light at the saturated intensity to obtain the rate at the maximum, and 0.5 mM P-*p*-BQ and 2 mM potassium ferricyanide were added. The reaction mixture contained 20 mM MES-NaOH (pH 6.5), 20 mM $CaCl_2$, 20 mM NaCl, 0.4 M sucrose, and the PSII complex or PSII−SBA conjugates equivalent to 3 μg of Chl/mL and phenyl-*p*-benzoquinone (P-*p*-BQ) as

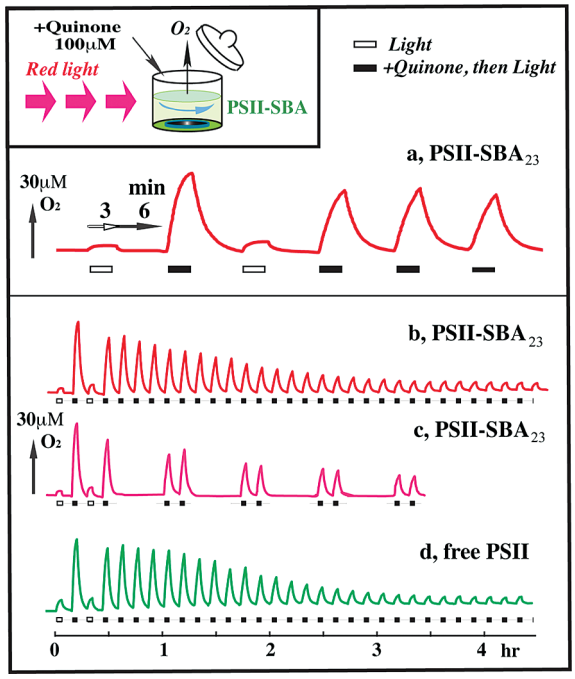

Figure 3. Light-induced oxygen evolution from the PSII−SBA_{23} conjugate and free PSII: (a−c) with PSII−SBA_{23} conjugates; (d) with free PSII. Changes in the concentration of oxygen were continuously monitored during the repetitive 3 min illuminations of red unsaturated intensity. Illuminations were done with and without addition of 0.1 mM P-*p*-BQ as indicated by the downward open and closed squares, respectively. P-*p*-BQ was added at 30 s before each illumination period as indicated. The reaction medium contained 20 mM MES-NaOH (pH 6.5), 20 mM $CaCl_2$, 20 mM NaCl, 0.4 M sucrose, and 2.3 mg/mL PSII−SBA_{23} conjugate that contains 0.09 μmol of PSII/mL. Inset: a schematic view of experimental system with a Clark-type electrode on the bottom of the vessel. A rid was opened during the dark intervals between the illumination periods to liberate evolved oxygen and to add P-*p*-BQ.

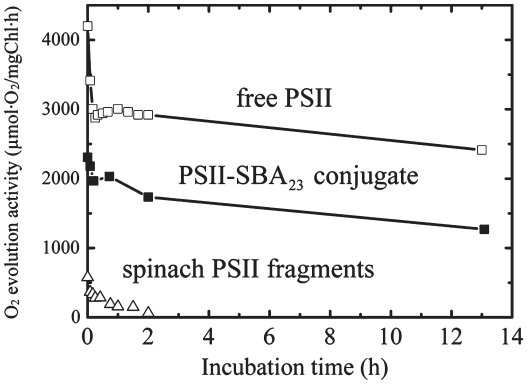

Figure 4. Time courses of decrease of oxygen evolving activity of PSII during the dark heat treatment at 40 °C. The activities of *T. vulcanus* PSII−SBA_{23} conjugate (close squares), free *T. vulcanus* PSII (open squares), and spinach PSII (open triangles) were measured at 25 °C after the varied lengths of heat treatment at 40 °C and following 10 min incubation at 0 °C as described in the Materials and Methods section.

Table 1. Oxygen Evolution Activity of PSII before and after Adsorption to SBA[a]

	oxygen evolution activity (% with respect to PSII in solution)
PSII in solution	100 ± 6
PSII−SBA_{23}	53 ± 3
PSII−SBA_{15}	32 ± 3

[a] The 100% activity corresponded to 4400 μmol of O_2/(mg of Chl h) measured at 25 °C of PSII in solution as described in the Materials and Methods section.

the external electron acceptor at 30 s before the onset of the excitation light. Evolved oxygen was released by opening the rid of vessel after each excitation period. The maximum oxygen evolution rate was calculated from the initial rate during the white-light illumination and was expressed in terms of mg of Chl, with an estimated error value of around 6%.

Assay of Thermal Stability of PSII. Thermal stability of free PSII and PSII−SBA_{23} conjugate were tested by measuring the oxygen evolution activity after varied lengths of heat treatment at 40 °C. Each sample was diluted with medium A to give a concentration of 0.1 mg of Chl/mL in a glass tube that was wrapped with aluminum foil and incubated at 40 °C for varied lengths of time. Then, the samples were rapidly cooled in an ice-containing water bath, incubated for 10 min, and subjected to the oxygen evolution measurement at 25 °C in a glass reaction vessel.

Purification of Spinach PSII Fragments. Oxygen-evolving PSII membrane fragments (spinach PSII) were prepared from spinach leaves as reported[33] with a slight modification.[34] The obtained PSII membrane fragments, which contain about 200 Chl *a* and Chl *b* per PSII, were suspended in a medium containing 50 mM MES-NaOH (pH 6.5), 20 mM NaCl, 1 mM EDTA, 0.4 M sucrose, and stocked in liquid N_2 until use. The oxygen evolution activity of spinach PSII was measured at a concentration equivalent to 15 μg of Chl/mL.

Results

Adsorption of PSII to SBA. Photographic images in parts D and E of Figures 1 represent dry powder of SBA_{23} before and after conjugation with PSII, respectively. The adsorption of PSII added a green color of Chl of PSII to SBA_{23}, and the color became more green, like the color of a plant leaf (not shown), if wet. Thus, we can directly detect the adsorption of PSII to SBA from the color change of SBA by the naked eye or by measuring the absorbance decrease of the supernatant solution after precipitating the PSII bound to SBA, hereafter designated as "PSII−SBA conjugate", by short centrifugation.

Figure 2 shows the time course of the adsorption of PSII to SBA. SBA dry powder was added at zero time to the solution containing PSII. The decrease in the absorbance at 673 nm of PSII in the supernatant was measured after precipitation of the PSII−SBA conjugate after varied incubation times. The rapid adsorption was detected within a few minutes after SBA_{15} or SBA_{23} was added to the PSII solution. In the case of SBA_{15}, the adsorbed amount reached a peak at 10 min (6.6 μg of PSII/mg of SBA_{15}) and then decreased to 4.7 μg/mg of SBA_{15} at 180 min. On the other hand, the adsorbed amount was 9.0 μg of PSII/mg of SBA_{23} at 10 min and gradually increased to 15 μg of PSII/mg of SBA_{23} at 180 min. The amount of PSII adsorbed to SBA_{23} after 3 h was 3 times larger than that adsorbed to SBA_{15} (Figure 2). The result indicates that PSII adsorption to SBA is sensitive to the pore size because SBA_{15} and SBA_{23} have similar particle sizes and physicochemical properties. The larger amount of PSII adsorbed to SBA_{23} suggests the binding into the inner pores.

We also performed N_2-adsorption isotherm measurements to determine the PSII adsorption. The fresh SBA_{23} showed an average pore diameter of 23 nm, as already mentioned, while pores were no longer available for N_2 adsorption after the treatment of SBA_{23} with a medium containing DM at 0.02% (w/v) or with a PSII solution containing DM at 0.02% (w/v), indicating that DM itself binds to the pores in SBA_{23}. Therefore, it was difficult to estimate the binding of PSII by this method, although the method has been successfully used to measure the bindings of bacterial membrane proteins.[14,15] PSII binding to SBA seems to occur in completion with DM that also binds to SBA. Similar, but weaker, competition between the protein complexes and other detergents were reported in the study of adsorption of LH2[14] and the bacterial reaction center complex to FSM.[15]

Oxygen Evolving Activity of PSII−SBA_{23} Conjugate. Oxygen-evolving activity of the PSII−SBA_{23} conjugate was measured with a Clark-type oxygen electrode system as shown in Figure 3 inset. Figure 3a shows the time course of the change of oxygen concentration upon the repetitive illumination cycles. The PSII−SBA_{23} conjugate was dispersed in a reaction medium inside a 1 mL vessel and illuminated for 3 min by the red illumination light followed by the 6 min dark interval. An artificial electron acceptor P-*p*-BQ was added to give a final concentration of 0.1 mM at 30 s before the illumination. Downward closed and open squares in traces a−d represent the illumination periods done with and without the P-*p*-BQ addition, respectively. In the first cycle in trace a, the PSII−SBA_{23} conjugate was illuminated without P-*p*-BQ, so that only a small change of oxygen concentration (including the artifact due to the temperature change by the illumination) was detected. In the second illumination, given in the presence of P-*p*-BQ, a larger increase of oxygen concentration from the original air-saturated level was detected. The rising rate slowed down at the end of the 3 min illumination. The peak level could be increased if we add the higher concentration of P-*p*-BQ. Then, the light was turned off, and the evolved oxygen was released into air by lifting a rid of the vessel. Upon the third illumination in trace a, which was done without the prior P-*p*-BQ supply again, almost no oxygen evolution was detected indicating the full consumption of oxidized form of P-*p*-BQ during the second illumination. The high oxygen productions were detected again as shown in the 4th−6th illumination periods which were done with the preadditions of P-*p*-BQ in each case. The results clearly indicate that PSII inside the PSII−SBA_{23} conjugate actively evolves molecular oxygen supported by the electron transfer from water to the external P-*p*-BQ as free PSII does in solution (see trace d).

Trace b of Figure 3 shows the same time course as trace a in a longer period. The peak height attained by the 3 min illumination decreased gradually, became almost a half that of the second one upon the 11th illumination (after 1.5 h from the start), and that upon the 32nd illumination (after 4.5 h) was almost null even with P-*p*-BQ. A similar time course (Figure 3, trace d) was obtained with the suspension of free PSII. If we compare the oxygen evolution activities (initial rates) upon the second illuminations in traces b and d, the activity in the PSII−SBA_{23} conjugate was 95% of that in free PSII. The activity of free PSII also decreased after 2−4 h measurement.

We, then, examined the effect of dark incubation length. Trace c of Figure 3 shows the experiment with the PSII−SBA_{23} conjugate similar to that in trace b, but with different dark intervals. After four cycles similar to those in trace b, the fifth illumination

(33) Berthold, D. A.; Babcock, G. T.; Yocum, C. F. *FEBS Lett.* **1981**, *134*, 231–234.
(34) Ono, T.; Inoue, Y. *Biochim. Biophys. Acta* **1986**, *850*, 380–389.

period was given after the longer dark time (27 min) by skipping three cycle times. The peak height attained by the fifth illumination was significantly lower than that of the fourth illumination, indicating the progress of inhibition even in the dark. However, the peak heights in the later cycles (e.g., after 3 h) were higher than those in traces b and d, indicating the suppressing effect of illumination.

The results in Figure 3 indicate that the PSII−SBA_{23} conjugate undergoes efficient electron transfer from water to added artificial electron acceptor P-*p*-BQ and evolves molecular oxygen in a rate comparable to that in free PSII for 2−3 h under the present experimental conditions (in which light intensity was attenuated to give one-third of the maximum rate that is described in the following section). Externally added P-*p*-BQ seemed to be almost freely accessible to PSII inside SBA_{23}. The activities of both PSII−SBA_{23} conjugate and free PSII decreased gradually as the increase of illumination period. The decrease seems to be induced by the illumination as well as the dark incubation with P-*p*-BQ.

Maximum Activity of Oxygen Evolution of PSII−SBA_{23} Conjugate. We also measured the oxygen evolution activity under very high (at a saturating intensity) white illumination light by omitting the red-pass filter emitting longer than 620 nm and a 10% neutral density filter from the illumination light source in the presence of higher concentration (0.5 mM) of P-*p*-BQ to measure the maximum ability for the first illumination period. The time course of oxygen evolution, as in Figure 3, under this condition indicated the evolution of 0.12 μmol of O_2/(mL min) in the medium containing 2.3 mg of PSII−SBA_{23} conjugates that contained 15 μg of PSII/mg of SBA_{23}. The rate was about 3 times higher than that seen in Figure 3. The concentration of PSII−SBA_{23} is equivalent to 3 μg of Chl *a* /mL (3 μmol of Chl *a*/mL which corresponds to 0.09 μmol of PSII/mL). The specific activity of O_2 evolution by the PSII−SBA_{23} conjugate on the Chl basis was calculated to be 2300 μmol of O_2/(mg of Chl h) (equivalent to 80 500 O_2 molecules/(PSII h) or 22 O_2 molecules/(PSII s)). The activity is higher than those at around 200−700 μmol of O_2/(mg of Chl h) of intact plants or isolated plant PSII membrane fragments that have higher numbers of antenna Chls associated with PSII (see Figure 4). We, thus, have produced PSII−SBA_{23} conjugates with the high specific oxygen evolving activity.

It is also interesting that the maximum activity of the PSII−SBA_{23} conjugate was 53% of free PSII under the saturating light intensity, while the activity measured under lower red light in Figure 3 was 95%. The results suggests that the activity of PSII adsorbed to SBA_{23} is limited by light intensity under the weaker red light and by some other factors, such as the diffusion of P-*p*-BQ, under the saturating white light that gave the 3 times higher activity in free PSII.

Thermal Stability. Figure 4 shows the effects of dark heat treatment at 40 °C (without P-*p*-BQ) on the oxygen evolving activities. Free PSII complex and PSII−SBA_{23} particles were incubated at 40 °C in the dark for varied lengths of times, incubated for 10 min at 0 °C, and then the oxygen evolving activities were measured at 25 °C in the reaction medium containing P-*p*-BQ under the saturating white light. Specific activities, expressed on Chl basis, of the PSII−SBA_{23} conjugate and free PSII were 4200 and 2400 μmol/(mg of Chl h), respectively, before the heat treatments. These activities were decreased to 2900 and 2000 μmol/(mg of Chl h), respectively, after the 20 min incubation at 40 °C, rather rapidly in both cases. Then, the activities decreased slowly and still maintained at 55% of the starting values even after the 13 h dark heat treatments in both cases.

Effects of 40 °C heat treatment on the spinach PSII membrane fragments are also shown by open triangles in Figure 4. The initial activity before the heat treatment was 580 μmol/(mg of Chl h). This low activity comes from the situation that the spinach PSII fragments contain the extra larger amounts of Chls on the Chl *a*/*b*−binding antenna protein complexes associated with the PSII reaction center complex to give the number of Chls per PSII to be around 200, in contrast to 35 in the purified PSII complex of *T. vulcanus* used in this study. The spinach PSII fragments were inactivated rapidly to 50% after the 15 min heat treatment and to 10% after the 2 h treatment even in the dark (Figure 4). The result indicates the higher heat stabilities of PSII and the PSII−SBA_{23} conjugate of *T. vulcanus* and that the PSII−SBA_{23} conjugate retained the high heat tolerance comparable to that of free PSII.

Distribution of PSII and a pH Indicator Dye Neutral Red (NR) inside SBA Measured by a Confocal Laser Scanning Microscope. We measured the distribution of PSII in SBA with a confocal laser scanning microscope. The stock solution of PSII−SBA conjugate or NR−SBA conjugate was diluted to give 0.2−0.4 mg of SBA/mL by dilution with medium A or 50 mM MES-NaOH (pH 6.5) buffer, respectively, and then 10 μL of each sample was mounted on a microscope slide and covered with a cover glass. The fluorescence intensities of PSII and of a small size molecule, neutral red (NR) bound to SBA particles were excited by a 488 nm laser beam. Figure 5 shows typical cross-section XY images of fluorescence intensities across single particles of PSII−SBA_{15} (A) and PSII−SBA_{23} conjugates (B) and NR−SBA_{15} (C) and NR−SBA_{23} conjugates (D). SBA_{15} and SBA_{23} particles had similar sphere sizes. The fluorescence of PSII Chl was high at the edge and was lower inside SBA_{23} (Figure 5B), while it was detectable only at the edge in SBA_{15} (Figure 5A). An inset at the bottom-right trace shows the profile of fluorescence intensity along the cross section indicated by a blue line in each image. Both the PSII−SBA_{23} and PSII−SBA_{15} particles gave sharp peaks at the surface. Only the PSII−SBA_{23} particles gave high Chl fluorescence inside. The fluorescence profiles along the cross section seemed to represent the PSII Chl distribution accurately because the fluorescence distribution along the *Z* axis showed profiles similar to those along the *x* or *y* axis (data not shown), indicating the low attenuation of intensities of fluorescence and excitation laser due to the self-absorption effects in the small SBA particles.

NR fluorescence, on the other hand, was almost equally distributed from the surface to the center in both the NR−SBA_{23} and NR−SBA_{15} conjugates. Fluorescence intensity was almost constant from edge to center in NR−SBA_{23} and was even higher at the center in NR−SBA_{15} (Figure 5, D and C, respectively). The amounts of NR adsorbed to SBA_{15} and SBA_{23} after 30 min incubations were 0.14 and 0.13 mg/mg of SBA, respectively, and did not change afterward. We also detected a slight release of NR from NR−SBA_{15} conjugates to the outer medium when we put the conjugates into the fresh medium. Therefore, the lower NR fluorescence on the edge of NR−SBA_{15} shown in the cross-section profile in Figure 5C seemed to occur through the release of NR from the edge moiety. No such release of PSII was detected, indicating the tighter binding of PSII. The flat intensity of NR fluorescence along the cross section shown by these images also suggest the low self-adsorption effect on the fluorescence intensity of NR inside SBA under the present condition.

To estimate the PSII contents at the surface and inside of SBA, we calculated the average intensity profiles of PSII fluorescence from the images shown in Figure 5 (along the cross sections at 12−16 radial angles) and then calculated the averaged profiles (see Figure 6). We also calculated the average external diameters of SBA_{15} and SBA_{23} to be 4.6 ± 1.4 and 4.7 ± 0.9 μm, respectively, based on microscopic images, such as those in Figure 5, of 101 and 89 particles of SBA_{15} and SBA_{23}. We simulated the concentration

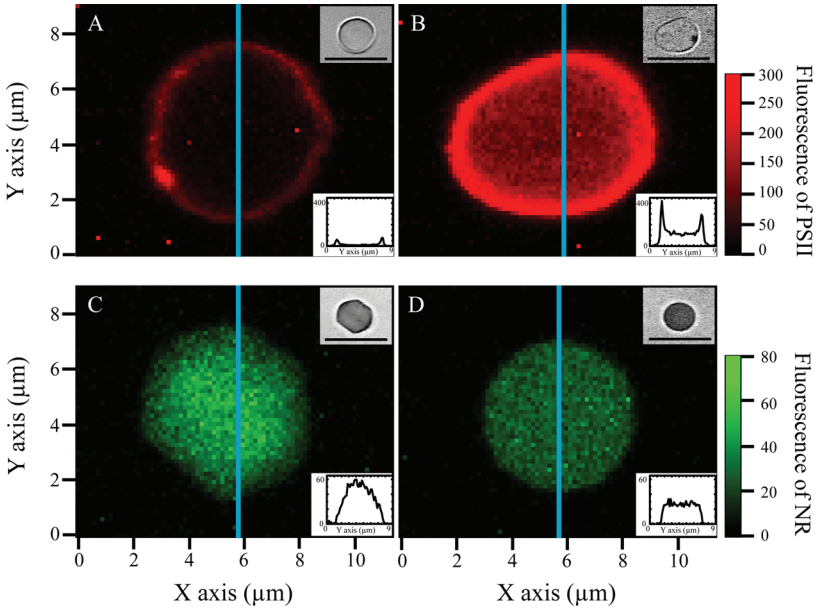

Figure 5. Confocal fluorescence images of PSII−SBA and NR−SBA conjugate single particles. Images in A, B, C, and D represent fluorescence from PSII−SBA_{15}, PSII−SBA_{23}, NR−SBA_{15}, and NR−SBA_{23} conjugate single particles, respectively, suspended in the reaction media. In (A) and (B), fluorescence intensities of chlorophylls of PSII were measured through a 650 nm red cutoff filter. In (C) and (D), NR fluorescence was measured without the cutoff filter. An inset at the upper right corner in each panel represents the microscopic image of a SBA particle. An inset graph at the lower right corner represents the fluorescence intensity profile of a cross section along the blue line. Each profile was calculated from the intensities at 0.75 μm width along the line. PSII and NR fluorescence intensities were excited by 488 nm excitation laser beam in medium A (pH 6.0) and 50 mM MES buffer (pH 6.5), respectively, as described in the Materials and Methods section.

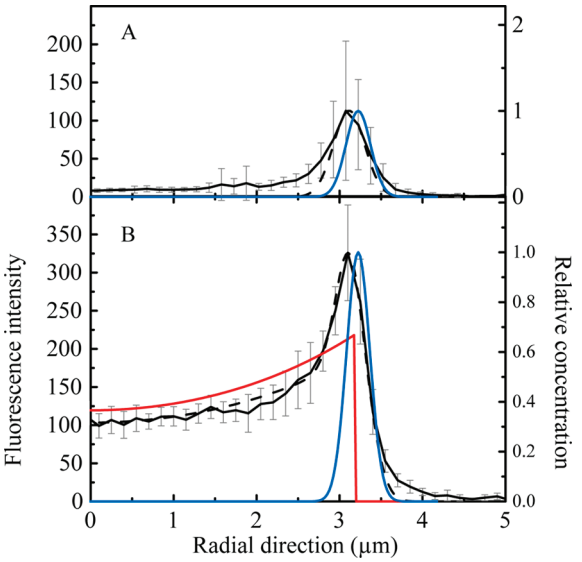

Figure 6. Cross-section profiles of the intensity of fluorescence of PSII−SBA single particles and simulated concentration profiles, respectively. (A) and (B): profiles across single PSII−SBA_{15} and PSII−SBA_{23} conjugate particles. Black solid lines in (A) and (B) show profiles of averaged fluorescence intensities calculated from the images of PSII−SBA_{15} and PSII−SBA_{23} conjugates in Figure 5, respectively. Black broken lines show the simulated curves. A red line in (B) represents the estimated PSII concentration (C_i) inside SBA_{23}. Blue lines in (A) and (B) represent the concentrations at the surface (C_s) of SBA_{23} and SBA_{15}, respectively, estimated as described in the text and Supporting Information.

profiles of PSII on PSII−SBA_{15} and PSII−SBA_{23} based on these experimental results, as described in the Discussion section.

Absorption and Fluorescence Spectra of PSII−SBA and NR−SBA Conjugates. Figure 7 shows the absorption and fluorescence spectra of PSII−SBA and NR−SBA conjugates.

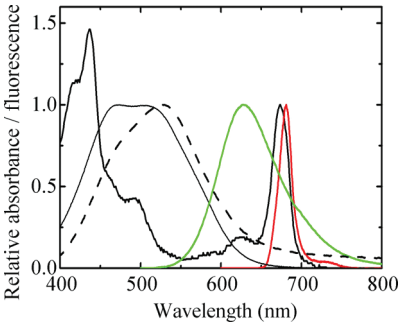

Figure 7. Absorption and fluorescence spectra of PSII−SBA_{23} and NR−SBA_{23} conjugates. A thick black solid line shows the absorption spectrum of PSII−SBA_{23} conjugates. Thin solid and broken lines show the absorption spectra of free NR and NR-SBA_{23} conjugates in a 50 mM MES-NaOH buffer (pH 6.5), respectively. The absorption spectra were corrected for the effect of light scattering from SBA by subtracting the spectrum obtained for SBA alone. Red and green solid lines show fluorescence spectra of PSII−SBA_{23} and NR−SBA_{23} conjugates, respectively.

The absorption (black solid line) and fluorescence emission (red line) spectra of PSII in the PSII−SBA_{23} conjugate could not be distinguished from those of the free PSII in solution, indicating the intact organizations of chlorophyll and the other pigments on PSII. Therefore, it is clear that the structure of PSII complex is almost preserved even after bindings to SBA. The decrease in the oxygen evolution activity, as shown in Figures 3 and 4, seems to come from the modification of the structure of the PSII complex in a moiety of the complex other than the pigment binding sites or due to some other factors, such as the slow diffusion rate of O_2 or P-*p*-BQ in the SBA nanopores.

Although the fluorescence spectrum of NR (green line) did not change upon the adsorption to SBA_{23}, its absorption spectrum

was changed by the adsorption to SBA, showing about a 20% increase of the shorter wavelength band compared to the NR in the outside medium (thin black line). The higher peak of the shorter wavelength band suggests the increase of protonated form of NR inside SBA that may reflect a negative 0.1−0.2 unit shift of the effective pH inside the SBA pores presumably due to the effects of immobilized SiO^- groups on the surface of nanopore walls. The shift, however, did not seem to affect oxygen evolution activity by itself in the reaction medium at pH 6.5 because the oxygen-evolving activity of PSII of *T. vulcanus* is reported to be almost independent of the medium pH at pH 6−7.[35−37]

Discussion

Adsorption of PSII into SBA. Various organic molecules and proteins have been adsorbed to mesoporous silica materials and found to be functional after adsorptions.[1] The larger and more hydrophobic membrane antenna pigment−protein complex LH2[14] and reaction center complex[15] of a thermophilic photosynthetic bacterium *Tch. tepidum* were also immobilized and stabilized by adsorption to FSM. Although the adsorption of these molecules into the nanopores has been confirmed by the decreased inner pore volumes measured in N_2 adsorption isotherm studies,[14,29] their distributions inside nanopores have not been clear. Recent technical advances have enabled the direct observation of the molecular distribution inside silica materials as fluorescence images detected by differential interference contrast microscopy or by confocal laser scanning spectroscopy.[9,11−13,38,39] We determined the distribution and functionality of PSII inside silica nanopores based on the confocal microscope measurement in this study.

PSII, which is a unique pigment−protein complex that extracts electrons from water using solar energy, evolves oxygen as a byproduct for the production of reducing power. The PSII complex that is insoluble in water can be extracted with full activity only with specific detergents. However, the plant PSII are rather fragile as shown for the spinach PSII membrane fragments in this study and the plant PSII reaction center complexes, which are comparable to the *T. vulcanus* PSII complex used in this study, are known to be more fragile and lose activity even at room temperature. The PSII complex purified from *T. vulcanus* gave the higher specific activity of oxygen evolution on SBA_{23} but not on SBA_{15}, indicating that only pores large enough to accept the 20 nm cylindrical structure can adsorb PSII dimer, as expected. The PSII−SBA_{23} conjugate with the high ability of oxygen evolution produced in this study can be a new material for the artificial photosynthesis if combined with a suitable energy-utilizing system. The method to hybridize biological and inorganic materials shown in this study will be useful for the artificial use of biological materials. We should solve the problem of gradual suppression by light and P-*p*-BQ to realize the much longer stable O_2 evolution.

Effects of Pore Size on the Adsorption of PSII to SBA. We used a confocal laser microscope for the direct measurement of the distributions of NR and PSII on SBA. The amounts of NR adsorbed to SBA_{15} and SBA_{23} were almost the same (0.14 and 0.13 mg/mg of SBA, respectively). NR penetrated into the inner spheres of both SBA_{23} and SBA_{15}. The results seem to indicate the relatively fast diffusion of small molecules into the nanopores inside SBA although the diffusion rate might vary depending on the molecular sizes and charges on the small molecules too. On the other hand, the amount of PSII adsorbed to SBA_{15} was only 31% of that adsorbed to SBA_{23} (Figure 2). The confocal images in Figure 5 showed that PSII was adsorbed to the surface of SBA_{15} and to both the surface and the inside of SBA_{23}. The time course of the binding of PSII to SBA_{23} showed fast (10 min) and slow (3 h) biphasic increases, while that to SBA_{15} occurred in a single fast phase (Figure 2). Thus, we assume that PSII was adsorbed rapidly to the surface of both SBA_{15} and SBA_{23} and slowly to the inner pores of the latter. The PSII concentration decreased from the edge to the center in SBA_{23}, probably due to the slow penetration rate of PSII inside the nanopores. The results are in line with the report on fluorescence-probe-labeled recombinant human interferon-α-2a, which slowly penetrated CM-Sepharose beads.[38]

Oxygen Evolution Activity of PSII−SBA Conjugates. The PSII−SBA_{23} conjugate showed high activity of oxygen evolution, as shown in Figure 3 and Table 1. The specific activities of PSII−SBA_{23} and PSII−SBA_{15} conjugates under high white saturating light based on chlorophyll contents were 53% and 32%, respectively, of that of free PSII measured in aqueous media (Table 1). The PSII on SBA_{15}, therefore, retained only 32% of its specific activity. On the other hand, PSII on SBA_{23} maintained higher (53%) specific activity even with the 3 times higher binding of PSII compared to that on SBA_{15}.

The fluorescence and absorption spectra of PSII bound to SBA_{23} and SBA_{15} were almost the same that in solution, suggesting almost no changes in the pigment organization. The result confirms the reports of LH2 and the reaction center complex of thermophilic photosynthetic bacterium *Tch. tepidum*.[14,15] These membrane−protein complexes were more stabilized inside FSM. On the other hand, the low 32% specific oxygen-evolving activity of the PSII−SBA_{15} conjugate suggests some alterations in the PSII structure upon the binding to SBA surface. Some modifications in the nonpigmented moiety (probably in the oxygen-evolving Mn complex) at the PSII surface may occur through binding to the SBA_{15} surface, as reported for some enzymes adsorbed to mesoporous materials.[7,8,40−42]

The oxygen-evolving activity of PSII in plants and cyanobacteria, except for thermophilic organisms, is known to be fragile and to be almost completely lost after a short incubation at 40 °C as shown for spinach PSII membrane fragments in Figure 4. It is probably due to the destruction of the Mn cluster.[24,43] On the other hand, PSII of *T. vulcanus*, which grows optimally at 57 °C, was highly stable. The ability of PSII is known to be preserved for more than a month even after crystallization.[32,44] The stability of PSII in SBA_{23} was almost the same as that of the free PSII of this organism because the activities of both PSII−SBA_{23} and free PSII were at 55−57% of the untreated ones even after 13 h at 40 °C (Figure 4).

We examined oxygen evolution activity of the PSII−SBA_{23} conjugate for a long period under the moderate intensity of red light that gave oxygen evolution activity of free PSII at ∼30% of the maximum obtained by the strong white saturating light. Repetitive illumination cycles produced oxygen from the PSII−SBA_{23} conjugate for a long period and the yield by each illumination

(35) Schiller, H.; Dau, H. *J. Photochem. Photobiol., B* **2000**, *55*, 138–144.
(36) Schlodder, E.; Meyer, B. *Biochim. Biophys. Acta* **1987**, *890*, 23–31.
(37) Shen, J. R.; Inoue, Y. *Biochemistry* **1993**, *32*, 1825–1832.
(38) Suh, C. W.; Kim, M. Y.; Choo, J. B.; Kim, J. K.; Kim, H. K.; Lee, E. K. *J. Biotechnol.* **2004**, *112*, 267–277.
(39) Wang, Y.; Angelatos, A. S.; Dunstan, D. E.; Caruso, F. *Macromolecules* **2007**, *40*, 7594–7600.
(40) Han, Y. J.; Watson, J. T.; Stucky, G. D.; Butler, A. *J. Mol. Catal. B: Enzym.* **2002**, *17*, 1–8.
(41) Yiu, H. H. P.; Wright, P. A.; Botting, N. P. *Microporous Mesoporous Mater.* **2001**, *44*, 763–768.
(42) Diaz, J. F.; Balkus, K. J. *J. Mol. Catal. B: Enzym.* **1996**, *2*, 115–126.
(43) Nash, D.; Miyao, M.; Murata, N. *Biochim. Biophys. Acta* **1985**, *807*, 127–133.
(44) Kern, J.; Loll, B.; Luneberg, C.; DiFiore, D.; Biesiadka, J.; Irrgang, K. D.; Zouni, A. *Biochim. Biophys. Acta, Bioenerg.* **2005**, *1706*, 147–157.

decreased to a half at the 12th cycle (at 100 min). About 3.3×10^3 oxygen molecules were evolved by one PSII reaction center within 20 times illumination period (180 min from the start). Thus, 1.3×10^4 electrons were transferred from water to P-*p*-BQ by red light illumination time of total 54 min per PSII.

In the reaction of oxygen evolution, water molecule should be oxidized in the four-electron reaction by the function of the manganese complex situated at the surface region of PSII complex. It is assumed that O_2 was evolved by the light reaction to give the electrons to the electron acceptor plastoquinone inside the PSII complex and then to the external electron acceptor P-*p*-BQ. Liberated oxygen should come out from SBA to the outer medium to be detected by the electrode. Reduced P-*p*-BQ also seems to come out too because we can assume almost full reduction of P-*p*-BQ in the medium after a few minutes illumination, as shown in Figure 3. In comparison to the activities in free PSII, the maximum activity of the PSII−SBA_{23} conjugate measured under the high white light was 53% (Table 1), and that under lower red light was 95% in Figure 3. These results suggests that the activity of PSII adsorbed to SBA_{23} is limited by light intensity under the weaker red light and by some other factors, such as diffusion of P-*p*-BQ or oxygen, under the saturating white light, although the precise diffusion rates of oxygen and P-*p*-BQ from SBA to outer medium are not known yet.

Concentration of PSII inside SBA_{23}. Assuming that PSII−SBA_{15} binds PSII only at the outer surface at a concentration C_s because of the high fluorescence only at the surface, we calculated the convolution integrals across a single SBA_{15} particle (broken lines in Figure 6) based on the particle size and the laser beam focusing size at $0.27 \times 0.27 \times 0.55\ \mu m^3$, as described in the Supporting Information. The calculated fluorescence profile showed a broad bandwidth and a peak shifted slightly to the inner side due to the convolution on the spherical SBA with a large beam size.

The cross-section profile of fluorescence across single PSII−SBA_{23} particle in Figure 5 was also simulated by assuming one more parameter, the inner concentration C_i. The C_i at a different spot inside SBA was calculated as the sum of the two exponential functions, each of which assumed monotonous exponential decay from one surface to the other, according to the equations in the Supporting Information. The parameters to determine C_i and C_s were then adjusted to set the convoluted profile to give the best fit to the experimental profiles. The best fit indicated that the total amounts of PSII (A_i and A_s) contributing to C_i and C_s were 59 and 41%, respectively (Table 2). Therefore, if we assume the same diameter sizes (4.6 μm) and numbers of particles per unit weight for SBA_{15} and SBA_{23} based on the measurement, 41% of PSII should bind to the SBA_{23} surface and the remaining 59% to the inside. The estimated A_s of 41% is higher than that on SBA_{15} because the latter A_s was only 31% of the total PSII amount (A_t) bound to SBA_{23}. If A_s is 41% in SBA_{23}, then the volume occupied by PSII dimers inside SBA_{23} becomes only 0.9% of the total pore volume of SBA_{23} (2.3 mL/g), with a calculated volume of $20 \times 13 \times 11\ nm^3$ for one PSII dimer. We also calculated the average distance between the PSII dimers to be 80 nm as schematically shown in Figure 1C. PSII will occupy 12% of the outer surface area on a single SBA_{23} (or SBA_{15}) particle with a radius of 2.3 μm, suggesting that PSII is adsorbed to the outer surface like in a monolayer.

Neutral red, a small pH indicator dye molecule, penetrated into SBA_{23} and SBA_{15} almost evenly from the surface to the center. Therefore, it is expected that PSII is adsorbed into SBA only when its molecular size is smaller than the pore diameter. It will be interesting to know how the diffusions of reactant/product molecules such as PSII, P-*p*-BQ, H_2O, H^+, or O_2 inside the nanopores regulate the activity.

Table 2. Estimated Amounts of PSII Bound to Different Parts of SBA and Their Specific Activities

	A_t total PSII amounts (specific activity)	A_s PSII at outer surface (specific activity)	A_i PSII inside (specific activity)
PSII−SBA_{15}	31 (32)	31 (32)	0
PSII−SBA_{23}			
case 1	100 (53)	41 (32)	59 (68)
case 2	100 (53)	41 (430)	59 (0)
case 3	100 (53)	31 (32)	69 (62)

Amounts of PSII on the surface and inside of SBA (A_s and A_i) were estimated from the PSII distribution measured by the confocal microscopy image in Figure 6 as described in the Supporting information. The amount at 100% corresponds to 15 mg of PSII/g of SBA. Numbers in parentheses indicate the relative activities of PSII oxygen evolution with respect to the activity in solution, which were estimated to interpret the activity of whole PSII−SBA conjugates in Table 1. See details about cases 1−3.

Activity of PSII inside SBA_{23}. If only the surface-bound A_s portion (41%) of PSII in SBA_{23} has a low 32% specific activity compared to the activity in solution, as seen with the A_s portion in SBA_{15}, then the A_i portion inside SBA_{23} (59% in amount) should show 68% specific activity to give the total activity of 51% (case 1 in Table 2). If we assume only the A_s portion to be active and the A_i portion to be inactive, then the A_s portion should have an unrealistic high specific activity of 430% (case 2). If A_s is 31%, as seen in SBA_{15}, we expect the specific activity of A_i portion to be 62% (case 3).

The estimations above indicate that the activity of PSII inside SBA_{23} is comparable (62 or 68% as estimated for cases 1 and 3) to that in the solution if we omit the unrealistic case 2. The result suggests the molecular environment inside nanopores in SBA to be almost the same as that in the outer medium. The result is in line with those estimated for the LH2 complex[14] and the bacterial reaction center complex[15] in FSM. In the latter case, FTIR spectrum of the reaction center complex in FSM was almost identical to that in solution.[15]

The hybridization of the bacterial protein complexes with FSM increased their heat stabilities,[14,15] while the heat stability of PSII was not markedly increased on adsorption to SBA, as seen in Figure 4. The activity of PSII was decreased by 68% by the adsorption to SBA surface. We assume that PSII structure was well maintained even inside the 23 nm silica pores of SBA_{23} and that the heat stability of oxygen evolving activity was not increased probably due to the unchanged stability of the Mn complex.

Conclusion

The PSII−SBA conjugate formed in this study has maintained the high and stable oxygen-evolving ability of *T. vulcanus* PSII even inside silica nanopores. The activity lasted more than 3 h under the moderate illumination/dark cycles. Future studies may further increase the stability. The conjugate will be a useful material for the construction of artificial photosynthetic systems. Combinations of the PSII−SBA conjugate with other membrane proteins, small water-soluble proteins, and different types of electron mediators are now under investigation. Concentrations of reactants and products in small silica tubes will be widely varied during the reactions. Combination of PSII−SBA conjugates with the mediator recycling systems, which can remove the harmful effects of electron acceptors and light-induced radicals, will allow us to produce oxygen and the reduced power continuously at the

same time. The method developed in this study will provide the basis for future hybridizations of biological complexes with artificial materials.

Acknowledgment. The authors thank Drs. Takumi Noguchi, Hiroyuki Mino, Yutaka Shibata, and Kouske Maki as well as Ms. Yoko Nakamura in the Department of Physics, Nagoya University, for their kind discussions and help during the work. We also acknowledge the support from Center for Gene Research, Nagoya University.

Supporting Information Available: Simulation of PSII concentration inside SBA_{23}. This material is available free of charge via the Internet at http://pubs.acs.org.